Moiré Interferometry for Microelectronics Packaging Interface Fatigue Reliability

Heng Liu[1], A.N. Cartwright[1], Cemal Basaran[1], William Casey[2]

[1]Electronic Packaging Laboratory, University at Buffalo, Buffalo, NY 14260;
Email: anc@eng.buffalo.edu; phone: (716) 6453115-1205.
[2]Quality and Reliability Assurance, Micron Technology Inc., Boise, ID; Email: wjcasey@micron.com .

Abstract

Moiré interferometry (MI) has been proven to be a very useful tool for testing the reliability of many different electronic packages. Historically, MI has been used for monotonic thermo-mechanical loading or steady-state conditions induced strain measurements but never for fatigue testing. Interface failure of microelectronics devices is a significant concern in packaging since it may cause a device to malfunction while in service. In this study, solder joint fatigue mechanisms, and their interfaces, are experimentally observed by means of a MI system. In addition, Scanning Electronic Microscopy (SEM) was also extensively utilized to support and document the MI observation. The combination of these two techniques and the robustness of the MI system is shown to be effective for the determination of the failure mechanisms of electronic packaging interfaces.

INTRODUCTION

Driven by trends toward miniaturization and higher levels of integration, the complexity of electronic packaging grows every day. High reliability of assembled components is critical to maintain a high level of final product quality. Ball Grid Array (BGA) and Fine Ball Grid Array (FBGA) packages are some of the most popular packaging technologies in the microelectronics industry due to the ever shrinking device size and increasing number of circuits and the corresponding increasing need for input/output interconnects for processors. These packages continue to be the technology of choice for both single and multi-chip module products.

The Pb/Sn eutectic solder alloy, which is highly studied and documented, is widely used as the joining material for BGA and FBGA packages in the electronic industry. It is well known that the dominant failure mode for solder joints is low cycle thermal fatigue caused by mismatches of the coefficient of thermal expansion (CTE) of the joined components. Thermally induced stresses within a package can be attributed to heat dissipated of high power densities during device operation.

Recently there has been an increasing interest in experimental analysis of solder joints and interfaces subjected to thermo-mechanical loading. Moiré interferometry, capable of providing whole field maps of deformation contour with sub-micron sensitivity, is extremely useful for studying thermo-mechanical behavior of electronic packaging structures[1-8,10].

In this study, MI allows measuring of the plastic strain field in a package during fatigue testing up to and including the failure point of the suspect area. The sensitivity of this advanced technique is typically 0.417µm. Through this technique, it is easy to pinpoint failure mechanisms and measure the plastic strain accumulation with micron accuracy. The technique also permits the pinpointing of the interfacial delamination point, along with the plastic strain field as a function of thermal cycles.

METHODOLOGY

The MI system used in this study has been described in detail in papers by Zhao[2,10] et. al. In this technique, a cross-line optical diffraction grating with 1200 lines/mm is replicated onto the specimen surface. The diffraction grating is illuminated by light from a He:Ne source laser, with a wavelength of 632 nanometers, which is split into four coherent beams (two vertical and two horizontal beams). The incident angle of these four coherent beams on the specimen grating is such that the ±1 diffraction orders emerge at an angle perpendicular to the specimen-grating surface. The diffracted beams then recombine in the direction normal to the specimen, and create interference patterns. Any deformation in the specimen surface deforms the optical diffraction grating and the resulting interference pattern (fringe pattern) of the diffracted beams changes. These fringe patterns represent the in-plane displacement contour maps. When the two vertical beams are blocked, the two horizontal beams interfere and generate a horizontal deformation field, called the U-field. Conversely, when the two horizontal beams are blocked, the two vertical beams interfere and generate a vertical deformation field, called the V-field.

The fringe patterns can be related to in-plane strains quantitatively as given by Post et al[1]:

$$\varepsilon_x = \frac{\partial U}{\partial x} = \frac{1}{f}\left[\frac{\partial N_x}{\partial x}\right] \qquad (1)$$

$$\varepsilon_y = \frac{\partial V}{\partial y} = \frac{1}{f}\left[\frac{\partial N_y}{\partial y}\right] \qquad (2)$$

$$\gamma_{xy} = \frac{\partial U}{\partial y} + \frac{\partial V}{\partial x} = \frac{1}{f}\left[\frac{\partial N_x}{\partial y} + \frac{\partial N_y}{\partial x}\right] \qquad (3)$$

where N_x is the horizontal fringe order and N_y is the vertical fringe order, ε_x. ε_y are normal strains and γ_{xy} is shear strain. In this project, the virtual grating frequency if f = 2400 lines/mm, corresponding to 1/f = 0.417 µms of sensitivity. Generally, we are interested in the failure mechanism of packages to thermal and vibrational loading. The temperature profile used in the study is shown in Figure 1a. The test was performed on five production quality FBGA specimens, each sample being thermally cycled up to 100 times. During the testing process each sample was measured with MI after every 20 thermal cycles.

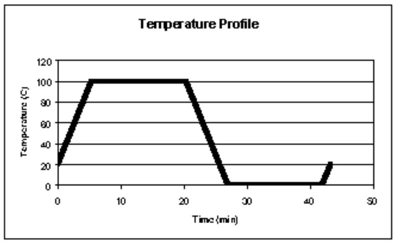

a. Temperature profile

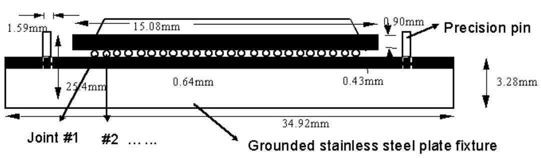

b. Specimen on fixture (not to scale)

Figure 1.Temperature Profile and Specimen on Fixture

The FBGA package has a typical sandwich structure, see Figure 1b. The component substrate is BT and the circuit board is a high Tg FR-4. The package size is 13x15 mm with 165 0.4 mm balls and a 5.95x11.11 mm die. The middle layer connecting the component to the circuit board is the eutectic 63Sn-37Pb solder joints. The boundary conditions used during testing simulated the actual boundary conditions found in a real life scenario by using a fixture with precision pins as shown in Figure 1b.

RESULTS

Using the strain-fringe relations given by Equation 1-3, strain can be calculated throughout the package, as shown in Figure 2.

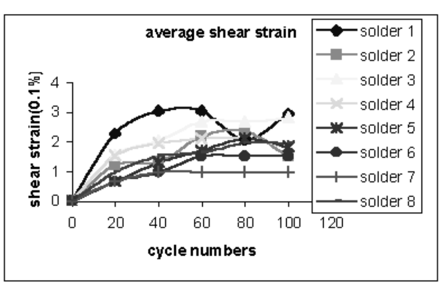

a.

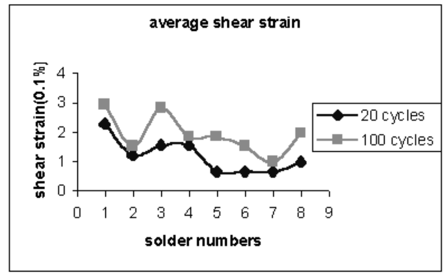

b.

Figure 2. Strain analysis

From Figure 2b, it is obvious that the strain distribution at 20 cycles and 100 cycles are quantatively different and that the distribution of strain has changed. This indicates that there is a formidable stress release in some of the solder joints due to interface failure. If there was not an interface (copper pad-PCB) failure, the factors affecting the distribution of the stress and strain in the solder joints show their influence at the very beginning and usually persist through the joint fatigue life, Zhao[2, 10] et al. Testing, if properly designed and conducted, should not alter such trends significantly enough to influence results. Therefore, improper packaging design or manufacturing process can usually be found within the early stages of thermal cycling. The general trend shown in Figure 2a is similar to earlier findings reported by Zhao[10] et al, which indicates that the plastic strain in the solder joint increases in the first forty cycles rapidly but then levels off and increases very slowly beyond that. This is probably due to the fact that Pb/Sn is a microstructurally evolving material[9]. As Pb/Sn alloy is cast it becomes a thermodynamically unstable material in a classic eutectic structure. With thermal cycling it evolves into a stable equiaxed grain structure, which continually coarsens. The coarsening process allows the solder to become more resistant to creep and plastic deformations. Therefore, after forty cycles the gradient of plastic strain increments reduces significantly albeit plastic strain continues to increase as cyclic loading continues.

The strain distribution shows that the maximum stress is experienced at the free edge solder joint or maximum distance from the neutral point (DNP). The plastic strain distribution usually follows the stress distribution hence the largest plastic strain is experienced at the free edge solder joint. Figure 2a indicates that the plastic strain increases in solder joint number 1, the leftmost in the package, up to the 60^{th} cycle and at the 80^{th} cycle the plastic shear strain and axial strain is smaller than at the 60^{th} cycle. This indicates that there is stress relaxation in the solder joint, possibly due to a crack initiation at the copper pad–PCB interface. This observation is also reinforced by fringe field figures, Figure 3a. It was observed that the change in shear strain (γ_{xy}) and axial strain (ε_x) from the 20^{th} cycle to the 100^{th} cycle was negligible; on the other hand the increase in peeling strain (ε_y) is significant. This is a good indicator for a delamination point. A close inspection of fringe fields indicates that at the

60th cycle and beyond fringes, which are continuous across the solder joint initially, become discontinuous at solder joint number one. After thermal cycling it is obvious that the fringes are no longer continuous across the solder joints near the free edge. This indicates that there is a physical discontinuity between the solder and joined layers. Moiré fringes can be thought of in the same manner as electrical potential, they must be continuous unless there is a discontinuity. If the bond between the solder bump and the joined layers remained continuous, the Moiré fringes would remain continuous across the interfaces, just the density of the fringes would increase in the solder joints, due to the CTE mismatch or boundary conditions.

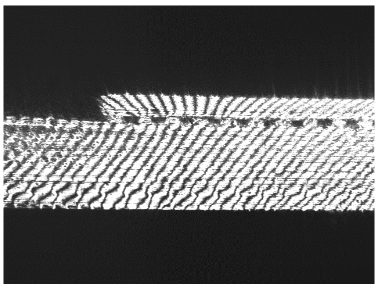

a. U-field Moiré

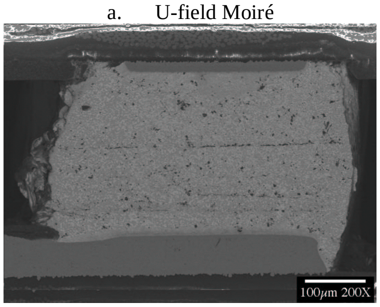

b. SEM

Figure 3. Solder one after 100 cycles

The original contribution of the technique developed in this study is that very often in new generation electronic packages the interface delamination point is not always known prior to testing due to heterogeneity of the system and initial defects due to manufacturing or defects in solder bumps and interfaces. A whole field optical fringe field approach detects any initiation of interface delamination immediately with great accuracy. This accuracy is dependent on the system sensitivity, and is defined by the frequency of the diffraction grating.

In the specific specimen studied here, the average inelastic strain value at the end of 100 cycles is rather small. This is due to proximity of the CTE between the bonded PCB layers and due to a weak bond between the solder pad and the upper PCB. A Scanning Electron Microscope (SEM) picture, Figure 3b, indicates that the bond between the upper PCB and copper pad becomes debonded after thermal cycling, which greatly reduces the shear stresses on the solder joints. This latter observation is quite consistent among all solder bumps that experienced the said interfacial delamination. Figure 3b shows that these solder joints really did not experience any increase in additional shear or axial plastic strain due to the additional thermal cycling conditions. However, it is also true that where there was no interfacial delamination inelastic shear and inelastic axial strain continued to increase. Once the interfacial delamination starts, the solder ball starts to experience stress relaxation. Therefore, the strain values are very consistent among all visible solder joints. Typically in BGA packages the failure occurs at the solder joint level, due to the cyclic shear strain it is subjected to and also due to it's low elastic modulus compared to other materials in the package. Also documented extensively is the fact that the intermetallics are usually much stronger than materials they interface with. Figure 3b, a picture of the 1st solder after 100 thermal cycles, indicates a debonding at this interface. The SEM pictures support the strain data obtained from MI test.

CONCLUSIONS

A Moiré interferometry technique was developed to study fatigue reliability of electronic packaging interfaces. Solder joints in the packages we tested exhibited classic BGA solder ball thermo-mechanical response. All strains in the solder joints were very small due to the minimal CTE mismatch between the joined PCB's and the failure and the crack initiation between the top copper pad an the top PCB layer. Because of the small creep strain levels, no failure was observed in any solder joint.

The MI measurements are supported by the SEM observations, which were also used to study failures that occurred in the interface between the component pad and the BT layer. We suspect that the failure is due to the imperfect initial bond between the copper pad and PCB, which is bonded by a resin epoxy and appears to be one of the weaker points in the package.

The temperature profile used in this testing is much higher than the service use environment, which also may have accelerated this interface degradation. Therefore, even if there is not a major problem with field failures, the partially bonded interfaces usually lead to reduced electrical performance primarily due to high electrical resistance in the interface. Consequently, being able to detect interface delamination with great accuracy, utilizing this advanced technology can be a valuable asset for microelectronic packaging designers and reliability engineers.

ACKNOWLEDGEMENTS

This research project is sponsored partially by a grant from National Science Foundation CMS Division Surface Engineering and Material Design Program under the supervision of Dr. Jorn Larsen-Basse, partially by a grant from the Office of Naval Research Advanced Electrical Power Systems program under the supervision of Dr. George Campisi and partially by Micron Technology Corp. Help received from Drs. Larsen-Basse and Campisi is gratefully acknowledged.

REFERENCES

[1] Post, D., Han, B. and Ifju, P. *High Sensitivity Moiré*, Springer-Verlag, 1994.

[2] Zhao, Y. Basaran, C. Cartwright, A. and Dishongh, T., *Thermomechanical Behavior Of Micron Scale Solder Joints Under Dynamic Loads*, Mechanics of Materials, Vol.32 Iss. 3, Feb. 16, 2000, pp. 161-173.

[3] Guo, Y. and Woychik, C.G., *Thermal Strain Measurements of Solder Joints in Second Level Interconnections Using Moiré Interferometry*, Journal of Electronic Packaging, Vol. 114, pp. 88-92, 1992.

[4] Guo, Y., Chen, W. T., and Lim, C.K., *Experimental Determination of Thermal Strains in Semiconductor Packaging Using Moiré Interferometry*, Proceedings of 1992 Joint ASME/JSME Conference on Electronic Packaging, American Society of Mechanical Engineers, New York, pp. 779-784, 1992.

[5] Han, B., *Recent Advancements of Moiré and Microscopic Moiré Interferometry for Thermal Deformation Analyses of Microelectronics Devices*, Experimental Mechanics, Vol. 38, pp. 278-288, 1998.

[6] Han, B. and Guo, Y., *Thermal Deformation Analysis of Various Electronic Packaging Products by Moiré and Microscopic Moiré Interferometry*, Journal of Electronic Packaging, Vol. 117, pp. 185-191, 1995.

[7] Post, D. and Wood, J. D., *Determination of Thermal Strains by Moiré Interferometry*, Experimental Mechanics, September, pp. 318-322, 1989

[8] Ratanawilai. T. B., Hunter, B., Subbarayan, G. and Rose, D., *A Comparison between Moiré Interferometry and Strain Gages for Effective CTE Measurement in Electronic Packages*, International Society Conference on Thermal Phenomena, Las Vegas, NV, pp. 246-252, 2000.

[9] Basaran, C. and Chandaroy, R., *Mechanics of Pb40/Sn60 Near Eutectic Solder Alloys Subjected to Vibrations*, Applied Mathematical Modeling, 22, 601-627.

[10] Zhao, Y., Basaran, C., Cartwright, A. and Dishongh, T., *Thermomechanical Behavior Of Micron Scale Solder Joints: An Experimental Observation*, Journal of the Mechanical Behavior of Materials, 1999, Vol.10, No.3, p.135-146.

ACRONYMS

MI: Moiré Interferometry
SEM: Scanning Electronic Microscopy
BGA: Ball Grid Array
FBGA: Fine Ball Grid Array
PCB: Printed Circuit Board
CTE: Coefficient of Thermal Expansion